Received: 18 June 2020 | Accepted: 23 November 2020

DOI: 10.1111/1365-2435.13728

RESEARCH ARTICLE

Functional Ecology | BRITISH ECOLOGICAL SOCIETY

Distinct carbon fractions drive a generalisable two-pool model of fungal necromass decomposition

Craig R. See[1] | Chris W. Fernandez[2] | Anna M. Conley[3] | Lang C. DeLancey[1] | Katherine A. Heckman[4] | Peter G. Kennedy[2] | Sarah E. Hobbie[1]

[1]Department of Ecology, Evolution, and Behavior, University of Minnesota, St. Paul, MN, USA

[2]Department of Plant and Microbial Biology, University of Minnesota, St. Paul, MN, USA

[3]Department of Chemistry, Carleton College, Northfield, MN, USA

[4]Northern Research Station, U.S. Forest Service, Houghton, MI, USA

Correspondence
Craig R. See
Email: crsee@umn.edu

Funding information
National Science Foundation (USA), Grant/Award Number: DEB-1234162, DEB-1754679 and DEB-1831944

Handling Editor: Pablo García-Palacios

Abstract

1. Fungi represent a rapidly cycling pool of carbon (C) and nitrogen (N) in soils. Understanding of how this pool impacts soil nutrient availability and organic matter fluxes is hindered by uncertainty regarding the dynamics and drivers of fungal necromass decomposition.
2. Here we assessed the generality of common models for predicting mass loss during fungal necromass decomposition and linked the resulting parameters to necromass substrate chemistry. We decomposed 28 different types of fungal necromass in laboratory microcosms over a 90-day period, measuring mass loss on all types, and N release on a subset of types. We characterised the initial chemistry of each necromass type using: (a) fibre analysis methods commonly used for plant tissues, (b) initial melanin and nitrogen (N) concentrations and (c) Fourier transform infrared (FTIR) spectroscopy to assess the presence of bonds associated with common biomolecules.
3. We found universal support for an asymptotic model of decomposition, which assumes that fungal necromass consists of an exponentially decomposing 'fast' pool, and a 'slow' pool that decomposes at a rate approaching zero. The strongest predictor of the fast pool decay rate (k) was the proportion of cell soluble components, though initial N concentration also predicted k, albeit more weakly. The size of the slow pool was best predicted by the acid non-hydrolysable fraction, which was positively correlated with melanin-associated aromatics. Nitrogen dynamics varied by necromass type, ranging from net N release to net immobilisation. The maximum quantity of N immobilised was inversely related to cell soluble contents and k, as positively related to FTIR spectra associated with cell wall polysaccharides.
4. Collectively, our results indicate that the decomposition of fungal necromass in soils can be described as having two distinct stages that are driven by different components of substrate C chemistry, with implications for rates of N availability and organic matter accumulation in soils.

KEYWORDS

carbon cycling, hyphal turnover, microbial biomass, nitrogen cycling, nitrogen immobilisation, soil carbon, soil organic matter

1 | INTRODUCTION

Dead microbial cells (i.e. necromass) often constitute more than half of the organic C and N in soils, with fungal necromass comprising the majority of this pool (Liang et al., 2019; Simpson et al., 2007). On short-term time-scales (e.g. days to weeks), the decomposition of fungal necromass is thus an important source of C and N to soil microbes and plants (Chen et al., 2019). Over longer time-scales, biomolecules from decomposing microbial necromass become stabilised to mineral surfaces, increasing long-term soil C storage (Cotrufo et al., 2013; Ludwig et al., 2015) and N retention (Fuss et al., 2019; Lovett et al., 2018). Despite its clear importance to the accumulation and availability of soil C and N, knowledge of the drivers and dynamics of fungal necromass decomposition is poor relative to understanding of senesced plant tissues.

There are growing calls for the explicit inclusion of microbial necromass into ecosystem models (e.g. Miltner et al., 2012; Simpson et al., 2007; Wieder et al., 2015). Previous studies have modelled fungal necromass decomposition as a uniform substrate with a constant decay rate (i.e. single exponential decay; Fernandez & Koide, 2014), which is how it has been treated in soil C models (Sulman et al., 2014, 2017). In reality, fungal necromass is a heterogeneous structure of biopolymers (e.g. polysaccharides, proteins, aromatic polymers) subject to degradation by different enzymes at different rates (Brabcová et al., 2016). This substrate heterogeneity is reflected in studies which suggest that fungal hyphae decompose in two distinct phases: an initial phase of rapid decomposition and a second phase of slow decomposition (e.g. Brabcová et al., 2016; Ryan et al., 2020; Schweigert et al., 2015). Recently, a 2-year study demonstrated that an asymptotic model of decomposition best described mass loss for four ectomycorrhizal fungal species (Fernandez et al., 2019). This model assumes that the fungal substrate consists of two distinct pools: a labile 'fast' pool that decomposes exponentially, and a recalcitrant 'slow' pool that decomposes at a rate approaching zero (Howard & Howard, 1974). If generalisable, this would provide useful parameters for incorporating fungal necromass into microbially explicit biogeochemical models, since a two-pool model of necromass decomposition implies distinct biochemical fractions with distinct implications for biogeochemical cycling. However, more observations are needed to determine whether the asymptotic model can be broadly applied across diverse fungal taxa.

Accurately modelling the dynamics and drivers of the early stages of fungal necromass decomposition (i.e. the fast pool) may be particularly important to soil N availability. Modelling N release from necromass is straightforward if treated as a homogeneous pool; a simple exponential decay rate dependent solely on N concentration results in species releasing N at a rate proportional to their mass loss. However, the presence of multiple N-containing pools which decay at different rates complicates this, especially if substrate N concentration is not the only driver of decay rate. Thus, while multiple studies have demonstrated that the early stages of fungal necromass decay are controlled in part by the N concentration (e.g. Fernandez et al., 2019; Koide & Malcolm, 2009), other chemical drivers (e.g. C quality) deserve further attention.

While fast pool necromass dynamics likely affect soil N availability, the size of the slow pool may affect long-term rates of C and N accumulation in particulate organic matter. This pool is thought to be composed of melanin located within the fungal cell wall (Fernandez et al., 2019). Among ectomycorrhizal fungi, melanised root tips persist longer in soil than non-melanised root tips (Fernandez et al., 2013), and melanised sclerotia can remain in soil for millennia (Scott et al., 2010). Recent field studies have linked melanised hyphae with SOM pools (Clemmensen et al., 2015; Lenaers et al., 2018; Siletti et al., 2017), suggesting an effect on soil C accumulation. The implications of a stable melanin-derived pool for soil N dynamics are less clear, as the chemical structure of many fungal melanin types do not contain N (Butler & Day, 1998). However, some fungal taxa produce melanin structures with N-containing indole groups (Eisenman & Casadevall, 2012), and N-containing proteins and chitin are often complexed with melanin in the cell wall (Butler & Day, 1998; Nosanchuk et al., 2015). These molecules could represent a previously overlooked pool of N immobilised in fungal necromass over long time-scales.

In the present study, we decomposed 28 field-collected fungal necromass types in laboratory microcosms containing non-sterile soils further inoculated with a ubiquitous soil saprotroph. Our primary objectives were to: (a) determine which commonly applied decomposition model best describes decomposing fungal hyphae across a phylogenetically and functionally diverse suite of taxa, (b) determine the biochemical components of fungal necromass most strongly associated with its decomposition dynamics and (c) determine how substrate chemistry and decay rate relate to the dynamics of N release during fungal necromass decomposition.

2 | MATERIALS AND METHODS

2.1 | Decomposition assay

Fresh sporocarps of 23 species of mycorrhizal and saprotrophic fungi were field harvested and oven dried at 45°C. The stipe was separated from the pileus in all samples where the two features were distinguishable. The pileus in mushrooms contains spores and tends to have higher C and N concentrations than the stipe (Hobbie et al., 2012), which we assumed to be chemically more similar to diffuse hyphae. Therefore, we discarded the pileus in all but five samples where we analysed it separately (n = 28 total samples). Substrates were oven dried at 50°C and ground to the consistency of fine sand in order to ensure a homogeneous sample for litterbags and chemical analyses.

We constructed five bags of each ground necromass type, each containing 85 ± 10 mg of dried fungal mycelium that was heat-sealed inside of two ~4 cm^2 squares made from 53 μm nylon mesh (Elko). Each bag was incubated in a 120-ml microcosm filled with ~80 ml live (i.e. unsterilised) mineral soil from the Cedar Creek Ecosystem Science Reserve, MN, USA. Upland soils at Cedar Creek are sandy Entisols, classified as Udipsamments (Grigal et al., 1974). Soils were

sieved to 2 mm and litterbags were deployed horizontally, with approximately 40 ml of soil above and below the litterbag. Microcosms were covered in clear plastic film, incubated in the dark at 20°C, aerated every 4–6 days, and soil moisture levels were maintained at 60% of field capacity until harvest. One bag of each necromass type was harvested after 2, 5, 8, 43 and 90 days of incubation.

Because a primary objective of this research was to compare the early stages of decomposition across substrates, we wanted to minimise differences due to the timing of saprotroph colonisation. Accordingly, we surface-inoculated all bags with a 50-µl slurry of water and hyphae from laboratory-cultured *Mortierella elongata* prior to incubation. *M. elongata* is a common saprotroph in soils globally (Li et al., 2018), plays a dominant role in microbial substrate decomposition (López-Mondéjar et al., 2018), and is an early coloniser of fungal necromass incubated in soils at Cedar Creek (Fernandez & Kennedy, 2018).

2.2 | Chemical analyses

We conducted a series of biochemical analyses to assess the initial substrate composition of all samples. We used forage fibre analysis, consisting of sequential extractions with neutral detergent, acid detergent and concentrated acid, to assess proximate carbon fractions of each fungal residue (ANKOM Technology). This procedure is commonly used in ecosystem studies to analyse plant tissues for decomposition studies (e.g. Hobbie et al., 2010; Wieder et al., 2009). To our knowledge this procedure has not yet been applied to fungal substrates, however, the carbon fractions it is meant to quantify in plants (e.g. cross-linked polysaccharide chains, proteins, amorphous aromatic polymers) are all present in fungi, and likely subject to degradation by similar classes of enzymes in soils (e.g. hydrolytic, proteolytic, oxidative). Briefly, cell soluble contents (e.g. simple carbohydrates, lipids, soluble proteins and non-protein N) were assessed as the amount of mass loss from each sample after gentle agitation in a neutral detergent for 75 min at 100℃. The residual material was agitated in an acid detergent (1N H_2SO_4) at 100℃ for 75 min to quantify the mass of amorphous glucan polymers (analogous to hemicellulose in plants) and bound proteins within the cell wall. Finally, the contents of acid hydrolysable cell wall components—likely crystalline glucans and chitin (Jang et al., 2004; analogous to cellulose in plants)—were determined with a 3-hr extraction in concentrated (72%) H_2SO_4 at room temperature with intermittent agitation. The remaining, acid unhydrolysable residues are thought to contain cell wall melanins (analogous to lignin) and other molecules complexed within them (Nosanchuk et al., 2015).

We quantified the relative proportion of various biochemical bonds present in the initial substrates using Fourier-transform infrared (FTIR) spectroscopy. Two milligram subsamples of each necromass sample were ground into a homogeneous powder with 100 mg KBr. Samples were pressed into a disc, and 64 transmission spectra scans were averaged across the 4,000–400 cm^{-1} range, at a resolution of 4 cm^{-1} using a Nicolet iS5 spectrometer fitted with an iD1 Transmission accessory (Thermo Fisher Scientific). Background subtraction was applied based on pure KBr spectrum, and a baseline correction factor was applied using OMNIC, version 9 (Thermo Fisher Scientific). Peak heights were *z*-score transformed prior to use in final analyses, and peaks corresponding to bonds in common biomolecules were identified based on previous characterisation (Table S1; Hribljan et al., 2017; Margenot et al., 2015).

In addition to the fibre fraction and FTIR spectral analyses, we measured total C and N concentrations and total melanin content. Per cent C and N were measured via dry combustion (Costech Analytical Technologies Inc.). Substrate melanin content was quantified using the commonly applied Azure A colorimetric assay (Fernandez & Koide, 2014). Briefly, 15 mg of ground sample was placed in 3 ml of Azure A solution (0.1M HCl mixed with Azure A dye to a 610 nm absorbance of 0.665) and incubated overnight. Melanin content was estimated as the decrease in 610 nm wavelength absorbance after incubation, based on a standard curve created using pure fungal melanin isolated from *Cenococcum geophilum* biomass.

We calculated net N immobilisation and release during the first 43 days of decay for 5 of the 28 necromass types, which were representative of the range in substrate quality (i.e. N and melanin concentrations). For each collection (2, 5, 8 and 43 days), we measured the N concentration of the necromass harvested from the bags. We estimated the proportion of the initial substrate N pool remaining for each bag at each collection time (Parton et al., 2007), such that $N_{retained} = (Mass_{final} \times [N]_{final})/(Mass_{initial} \times [N]_{initial})$, where $N_{retained}$ represents the proportion of the initial N pool remaining, $[N]_{initial}$ and $[N]_{final}$ represent the respective substrate N concentrations and $Mass_{initial}$ and $Mass_{final}$ represent the respective masses of substrate in the litterbags. Values greater than 1 indicate net immobilisation, whereas values less than 1 indicate net release. Due to differences in the timing of N release and the magnitude of N immobilised when N release began among substrates, we calculated the maximum level of immobilisation (across all collections) for each necromass type.

2.3 | Statistical analysis

We compared the single exponential decomposition model of the form $X = e^{-k_s t}$, where X is the proportion of the mass remaining at time t (in days) and k_s is the decay rate, to the asymptotic model of the form $X = A + (1 - A)e^{-kt}$, where k is the decay rate of the fast pool and A is the size of the slow pool which decomposes at a rate of zero (in reality, the decay rate of the slow pool is likely very close to, but not equal to, zero). We fit these models to the proportion mass remaining for each substrate across the five harvest times (Howard & Howard, 1974; Olson, 1963). We also attempted to fit the data to a double exponential model, which assumes that both the fast and slow pools decay exponentially at different rates (Lousier & Parkinson, 1976); however, these models did not

converge. We compared the fits of the single and asymptotic models based on the root sum of squares, and the corrected Akaike's information criterion (AICc) values. We used ANOVA to compare the differences in decomposition parameters for the substrates categorised by trophic mode (mycorrhizal, soil saprotroph, wood saprotroph), taxonomic order and sporocarp component (stipe vs. spore-bearing).

To assess the effects of substrate chemistry on decomposition dynamics, we used the parameters from the decomposition models (decay rate *k* and slow pool size *A*) as dependent variables in multiple linear regression analyses, with substrate chemical concentrations as explanatory variables. Because the fibre fractions sum to 100%, using multiple fractions as predictors would violate the assumption of independence required for multiple regression. To avoid issues of collinearity among predictors, we compared these fractions to the dependent variables separately using simple linear regression, and then included only the best predictor in the larger model. For similar reasons, we chose to include substrate N concentration, but not C:N ratio in our pool of explanatory variables – substrate C:N was highly correlated with per cent N, but less correlated than N with our dependent variables (Table S2). Starting with a model that included N concentration, melanin concentration N, one fibre fraction and all possible interactions, we used a backward-selection stepwise procedure to select the best model based on AIC. We qualitatively described the biochemical bonds associated with the C and N fractions using Pearson correlations with the peaks obtained from FTIR spectra. Finally, we used *k* and the chemical variables found to predict it as explanatory variables in simple linear regressions to predict N immobilisation (calculated as the maximum proportion of initial N remaining across collections).

3 | RESULTS

The asymptotic model of decomposition consistently fit the mass loss data better than the commonly used single exponential model, as evidenced by a lower residual sum of squares in all 28 models (Table 1). The AIC values were also lower for the asymptotic models than the single exponential models in all but one time series (*Laetiporus sulphureus*; Table 1). We found considerable variation in the fast pool decay rate across substrates (*CV* = 34%), with *k*-values ranging from 0.07 to 0.35 per day. We found even higher variation in the asymptotic fraction (*CV* = 41%), with *A*-values ranging from 0.04 to 0.26. These parameters appeared to be independent from each other, as *A*-values and *k*-values were not significantly correlated in this dataset ($R^2 = 0.06$, $p = 0.20$, Table S2). Variation in *k* and *A*-values was not well explained by trophic mode or sporocarp component, though we found differences between taxonomic orders (Figure S3).

Variation in the *k*-values associated with the fast pool from the asymptotic model was explained by initial substrate chemistry. The most parsimonious model based on stepwise AIC selection contained only the soluble cell contents and N concentration as explanatory variables with no interaction (*k*-value = −0.1417 + 0.0043 × CellSolubles + 0.0088 × PercentN; Table S4). Cell soluble components, acid detergent and acid hydrolysable fractions all predicted *k* when considered independently (Figure 1). Of these, the strongest predictor of decomposition rate was cell soluble components, which increased with *k* ($R^2 = 0.56$, $p < 0.001$; Figure 1). Initial N concentration also predicted the decomposition rate of the fast pool ($R^2 = 0.19$, $p = 0.02$; Figure 1), and was not correlated with cell soluble components or any other fibre fraction (Table S2).

The *A*-values representing the size of the slow pool from the asymptotic model were explained by melanin concentration and the acid non-hydrolysable fraction. The most parsimonious model based on the stepwise AIC procedure contained only these two variables with no interaction (*A*-value = 0.1378 + 0.0056 × Melanin + 0.0055 × Non-hydrolysable; Table S4). Melanin and the non-hydrolysable fraction also significantly predicted the *A*-value in simple linear regression (Figure 2), however, these relationships were driven by the upper half of these substrate concentrations (Figure S5).

Peaks from the FTIR spectra corresponded to substrate chemistry measurements and decomposition model parameters (Table 2). The two alcohol (R-OH) peaks (1,080 and 1,160 cm^{-1}) had strong negative correlations with the two best predictors of fast pool decay rate: peak 1,080 cm^{-1} was inversely correlated with N concentration, and peak 1,160 cm^{-1} was inversely correlated with cell soluble contents. Consequently, these R-OH peaks were associated with lower *k* values in the fast decomposing pool (Table 2). Both amide bond peaks (1,550 and 1,650 cm^{-1}) were highly indicative of N concentration, and also correlated with the fast pool decomposition rate. The two peaks thought to be associated with fungal melanins (840 and 1,234 cm^{-1}), however, corresponded to different biochemical fractions. The 1,234 cm^{-1} ester peak was associated with the non-hydrolysable fraction and melanin contents, which in turn were correlated with the size of the slow pool (*A*-value). Surprisingly, the 840 cm^{-1} aromatic peak was negatively related to total C, and was not associated with melanins, but rather was positively related with cell-soluble contents. Aliphatic peaks were positively correlated with the non-hydrolysable fraction and melanin contents (Table 2), but these relationships were strongly driven by a single point (Figure S6).

Nitrogen release during decomposition differed among the five necromass types examined (Figure 3a). Necromass types with the lowest initial N concentrations (3.2% N in both *Camarops petersii* and *Grifola frondosa*) both displayed net immobilisation of N by the second day of decomposition (Figure S7). Notably, *C. petersii* necromass more than doubled its N content during the first 48 hr of decomposition. Similarly, *G. frondosa* N content increased 30% after losing 40% of its mass (Figure S7). In contrast, necromass types with the highest initial N concentrations exhibited immediate declines in N content. Nitrogen immobilisation (measured as the maximum proportion of initial N) was negatively related to decay rate of the fast pool ($R^2 = 0.81$, $p = 0.04$, Figure 3b). As cell soluble contents increased,

TABLE 1 Model parameters and fit statistics for two decomposition models describing mass loss for 28 types of fungal necromass. k_s = exponential decay rate from single pool model, k = exponential decay rate from asymptotic model, A = size of remaining 'slow pool' after exponential phase (asymptotic model only), AIC = corrected Akaike information criterion score, RSS = Root sum of square error for model

Necromass type				Single exponential model			Asymptotic model			
Species	**Tissue**	**Order**	**Trophic Mode**	k_s	**AIC**	**RSS**	A	k	**AIC**	**RSS**
Lactarius vinaceorufescens	Stipe	Russulales	Mycorrhizal	0.03	−15.24	0.014	0.15	0.04	−21.17	0.004
Laetiporus sulphureus	Sporocarp	Polyporales	Wood rotter	0.03	−10.52	0.031	0.07	0.04	−8.85	0.029
Camarops petersii	Sporocarp	Boliniales	Wood rotter	0.02	−7.50	0.052	0.35	0.06	−31.89	0.001
Laccaria laccata	Stipe	Russulales	Mycorrhizal	0.03	−4.15	0.090	0.22	0.08	−4.38	0.062
Lactarius chelodonius	Stipe	Russulales	Mycorrhizal	0.05	−6.10	0.065	0.19	0.09	−8.88	0.029
Scleroderma citrinum	Sporocarp	Boletales	Mycorrhizal	0.04	−2.74	0.114	0.29	0.09	−14.98	0.011
Russula emetica	Cap	Russulales	Mycorrhizal	0.06	−4.70	0.082	0.22	0.11	−16.24	0.009
Rhizopogon ochraceorubens	Sporocarp	Boletales	Mycorrhizal	0.08	−4.37	0.087	0.14	0.11	−4.81	0.058
Macrolepiota procera	Cap	Agaricales	Soil saprotroph	0.10	−6.61	0.060	0.13	0.12	−8.76	0.030
Suillus grisellus	Stipe	Boletales	Mycorrhizal	0.06	−3.61	0.099	0.23	0.12	−9.51	0.026
Boletus pseudosensibilis	Stipe	Boletales	Mycorrhizal	0.06	−3.13	0.107	0.23	0.12	−8.09	0.034
Gomphidius glutinosus	Stipe	Boletales	Soil saprotroph	0.07	−3.16	0.107	0.21	0.12	−7.02	0.040
Russula emetica	Stipe	Russulales	Mycorrhizal	0.07	−3.64	0.098	0.24	0.12	−14.45	0.012
Suillus viscidus	Stipe	Boletales	Mycorrhizal	0.09	−4.96	0.079	0.15	0.13	−6.76	0.042
Tricholoma spp	Stipe	Agaricales	Mycorrhizal	0.05	−2.40	0.121	0.25	0.13	−8.42	0.032
Hygrophorus paludosoides	Stipe	Agaricales	Soil saprotroph	0.07	−2.38	0.121	0.20	0.13	−4.31	0.063
Lactarius chelodonius	Cap	Russulales	Mycorrhizal	0.07	−3.83	0.095	0.21	0.13	−9.91	0.025
Leccinum aurantiacum	Stipe	Boletales	Mycorrhizal	0.09	−0.73	0.160	0.19	0.15	−1.35	0.103
Grifola frondosa	Sporocarp	Polyporales	Wood rotter	0.13	−5.54	0.072	0.11	0.16	−5.86	0.049
Suillus spectabilis	Stipe	Boletales	Mycorrhizal	0.12	−8.36	0.045	0.13	0.16	−14.80	0.011
Macrolepiota procera	Stipe	Agaricales	Soil saprotroph	0.13	−2.62	0.117	0.13	0.17	−2.68	0.083
Hygrocybe punicea	Stipe	Agaricales	Soil saprotroph	0.13	−5.73	0.069	0.15	0.19	−9.41	0.027
Boletus pseudosensibilis	Cap	Boletales	Mycorrhizal	0.15	−7.26	0.054	0.13	0.19	−10.73	0.022
Polyporus squamosus	Sporocarp	Polyporales	Wood rotter	0.17	−8.22	0.046	0.08	0.20	−8.25	0.033
Boletus campestris	Stipe	Boletales	Mycorrhizal	0.15	−4.38	0.087	0.18	0.22	−9.73	0.026
Chlorophyllum molybdites	Stipe	Agaricales	Soil saprotroph	0.14	−3.26	0.105	0.22	0.23	−13.23	0.014
Suillus spectabilis	Cap	Boletales	Mycorrhizal	0.17	−7.17	0.055	0.14	0.24	−12.23	0.017
Chlorophyllum molybdites	Cap	Agaricales	Soil saprotroph	0.17	−3.85	0.095	0.18	0.26	−8.04	0.034

the maximum proportion of N immobilised decreased (R^2 = 0.91, p = 0.01), with necromass types with the highest concentrations of cell solubles releasing N immediately (Figure 3c). Conversely, we found a strong positive relationship between the maximum quantity of N immobilised and the R-OH bond contents of the initial substrate (R^2 = 0.96, p = 0.003, Figure 3d).

4 | DISCUSSION

4.1 | A generalisable two-pool model of fungal necromass decay

Our results demonstrate broad support for the asymptotic model in describing the decomposition of fungal necromass in soils. In this model, a fast pool decomposes exponentially on the order of days to weeks, followed by a slow pool that decomposes at a rate approaching zero. This model has been used extensively to characterise plant tissue decomposition (Berg, 2000; Wieder & Lang, 1982), but with the fast pool in plants decomposing orders of magnitude more slowly than fungal necromass (i.e. measured in years, not days). The size of the slow pool across fungal species (7%–35%, mean = 18%) was smaller and less variable than those observed in leaf litter (e.g. 5%–49%, mean = 29%; Berg, 2000). The length of our study did not allow us to quantify the long-term decomposition dynamics of the slowly decomposing necromass pool. Moving forward, multi-year studies are needed to better characterise the decay rate of the slow fraction of fungal necromass.

Our study examined the dynamics and drivers of the fast pool across phylogenetically diverse fungi. We found a wide range in C and N fractions among the necromass types analysed (Table S8), corresponding to different bonds in the FTIR spectra (Table 2).

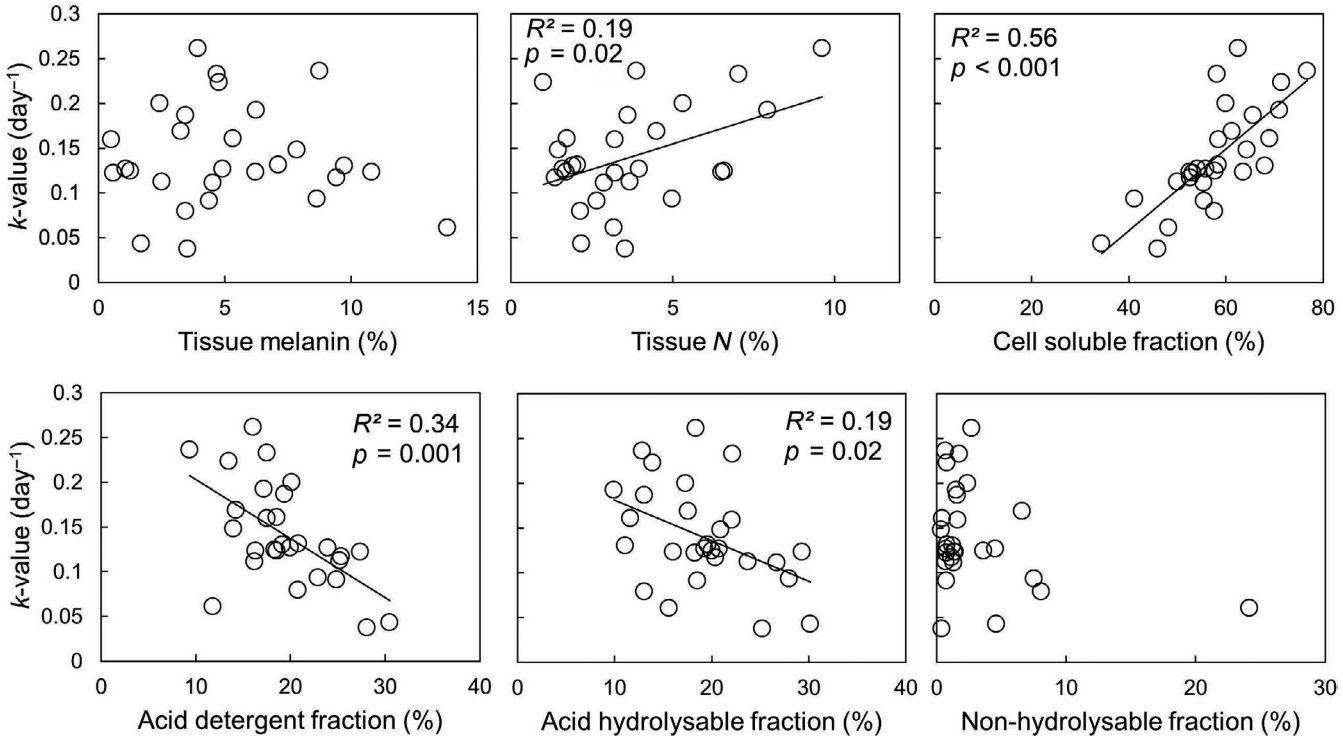

FIGURE 1 Relationships between fast pool decay rates (i.e. *k*-values from the asymptotic models) and initial substrate chemistry for the 28 fungal necromass types

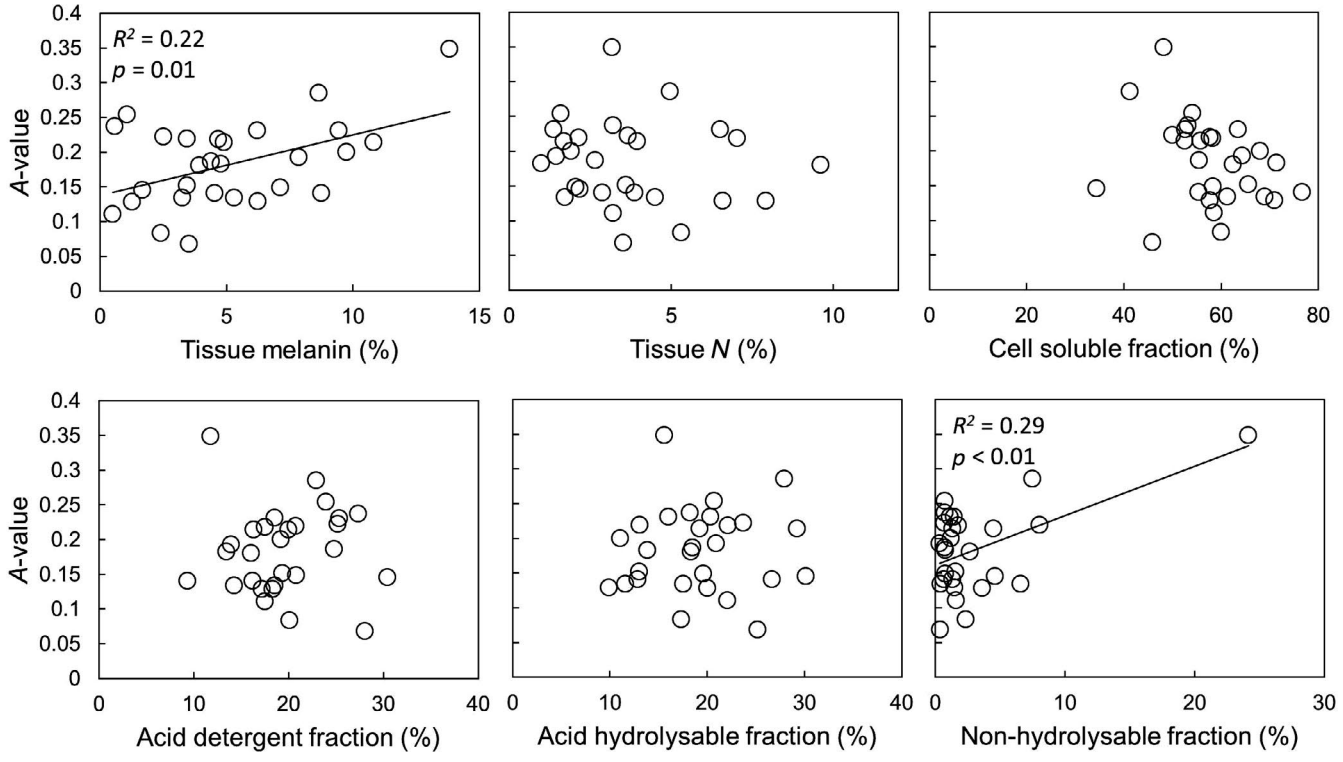

FIGURE 2 Relationships between slow pool size (i.e. *A*-values from the asymptotic models) and initial substrate chemistry for the 28 fungal necromass types

Prior studies have related N concentration to early stages of necromass decomposition (e.g. Fernandez & Koide, 2014; Koide & Malcolm, 2009; Maillard et al., 2020; Ryan et al., 2020), but have largely overlooked the importance of carbon fractions in these substrates. We found cell-soluble contents to be the strongest predictor of *k*, independent of substrate N concentration. This observation,

TABLE 2 Pearson's correlation coefficients between chemical fractions and normalised FTIR peaks for 28 fungal necromass types. Columns reflect FTIR wavenumber and the corresponding organic functional group. *A* and *k* are parameters from an asymptotic decomposition model. All chemical and fibre fractions were calculated as a percentage of dry mass. Bold, italicised values denote statistical significance at $p < 0.10$, '*' denotes $p < 0.05$, '**' denotes $p < 0.01$ and '***' denotes $p < 0.001$

	Aromatic		Amide		Alcohol		Aliphatic		Alkene
	840	1,234	1,650	1,550	1,080	1,160	2,850	2,924	920
A	−0.21	***0.35***	−0.07	0.02	0.18	0.13	***0.33***	***0.35***	−0.02
K	0.23	−0.16	***0.47****	***0.45****	***−0.40****	***−0.69*****	−0.16	−0.20	−0.11
Total N (%)	−0.13	***0.33***	***0.83*****	***0.80*****	***−0.70*****	−0.28	***0.37***	***0.34***	***−0.32***
Melanin (%)	0.07	***0.37****	−0.10	−0.03	0.01	0.02	***0.30***	***0.39****	−0.09
Total C (%)	***−0.41****	***0.56*****	0.27	0.21	***−0.58*****	−0.18	***0.72*****	***0.78*****	***−0.53*****
Cell soluble components (%)	***0.44****	−0.17	0.22	0.26	−0.23	***−0.63*****	−0.27	−0.22	0.06
Acid detergent fraction (%)	−0.21	−0.16	−0.28	−0.33	***0.34***	***0.42****	−0.13	−0.20	0.16
Acid hydrolysable fraction (%)	***−0.44****	−0.05	−0.22	−0.24	0.18	***0.45****	0.15	−0.01	−0.15
Non-hydrolysable fraction (%)	−0.14	***0.5*****	0.11	0.13	−0.12	0.27	***0.50*****	***0.65*****	−0.13

along with the negative relationships observed between *k* and the more recalcitrant fractions of our assay, supports the idea that the size and C chemistry of the fungal cell wall determines *k* for the fast pool (Fernandez et al., 2016). This is further supported by the strong inverse correlation between *k* and R-OH functional groups from the FTIR analyses, as these groups are present in high quantities in the polysaccharides (β-glucan, chitin) composing the cell wall (Table 2). While the fast fraction represented the majority of the initial substrate across our dataset (65%–93% by mass), our use of freshly killed hyphae may overestimate the relative proportion of the fast pool in situ, since some of it is likely reabsorbed by the fungi during hyphal senesce (Boberg et al., 2014). Importantly, the half-life of the fast pool fraction varied by a factor of 6 (range = 3–18 days) across these species, suggesting that differences in fungal community composition can result in important differences in C and nutrient availability to soil.

4.2 | Drivers of N retention during necromass decomposition

Our results highlight considerable variation in N release among fungal necromass types during the early stages of decomposition. Despite substantial mass loss from all necromass types in the first 8 days of decomposition, N dynamics ranged from net release to net immobilisation of N during this time (Figure 3a). Substrates with the highest initial N began losing N immediately, while lower-N substrates remained a net sink for N until the majority of mass loss had occurred (Figure S7). This pattern mirrors observations in plant litter in many ecosystems (Parton et al., 2007), but over a much shorter time-scale. Interestingly, initial N concentrations were not the best predictors of initial N release, and did not significantly correlate with the rates of immobilisation (Figure S7), though the limited sample size of this analysis only allowed for detection of strong trends. Instead we found that N retention in fungal necromass was well predicted by *k*, and the substrate C chemistry driving *k* (Figure 3b,c,d).

Differences in N release among necromass types likely reflect variation in the size and composition of the cell wall, with more N immobilisation in taxa with more cell wall polysaccharides (i.e. R-OH groups; Figure 3d). In contrast to N contained within the cell soluble fraction, N complexed as proteins within the cell wall or contained within acetylglucosamine monomers of chitin require enzymatic attack to be released. Both cell wall components and R-OH bond content were inversely correlated with *k* (Figure 1, Table 2), reflecting rate limitation of the hydrolytic enzymes responsible for degrading the polysaccharides within this pool (Sinsabaugh et al., 2002). This is consistent with the findings of Fernandez and Koide (2012), who found that chitin losses from decomposing necromass were much greater during the second half of a one-month incubation. This suggests that rates of N release from the fast decomposing pool of fungal necromass will be determined by the ratio of N contained in the cell-soluble fraction to N incorporated within the cell wall. Fungal cell walls vary considerably in size, and contents of chitin and glycoproteins (Bowman & Free, 2006). Ecologically, this implies that factors affecting the cell wall traits of soil fungi (e.g. environmental stress, species turnover) may have considerable afterlife effects on rates of soil N availability. Future field studies are needed to confirm this hypothesis.

4.3 | Implications of a two-pool model for soil carbon storage

Both fast and slow decomposing pools of fungal necromass are likely to affect rates of SOM accumulation, but through different mechanisms. The fast fraction will directly contribute to mineral-stabilised SOM formation insomuch as low-molecular weight components (e.g. amino sugars, lipids) released during decomposition are directly sorbed to mineral surfaces (Miltner et al., 2012; Shao et al., 2019). This pool may also affect rates of C stabilisation by

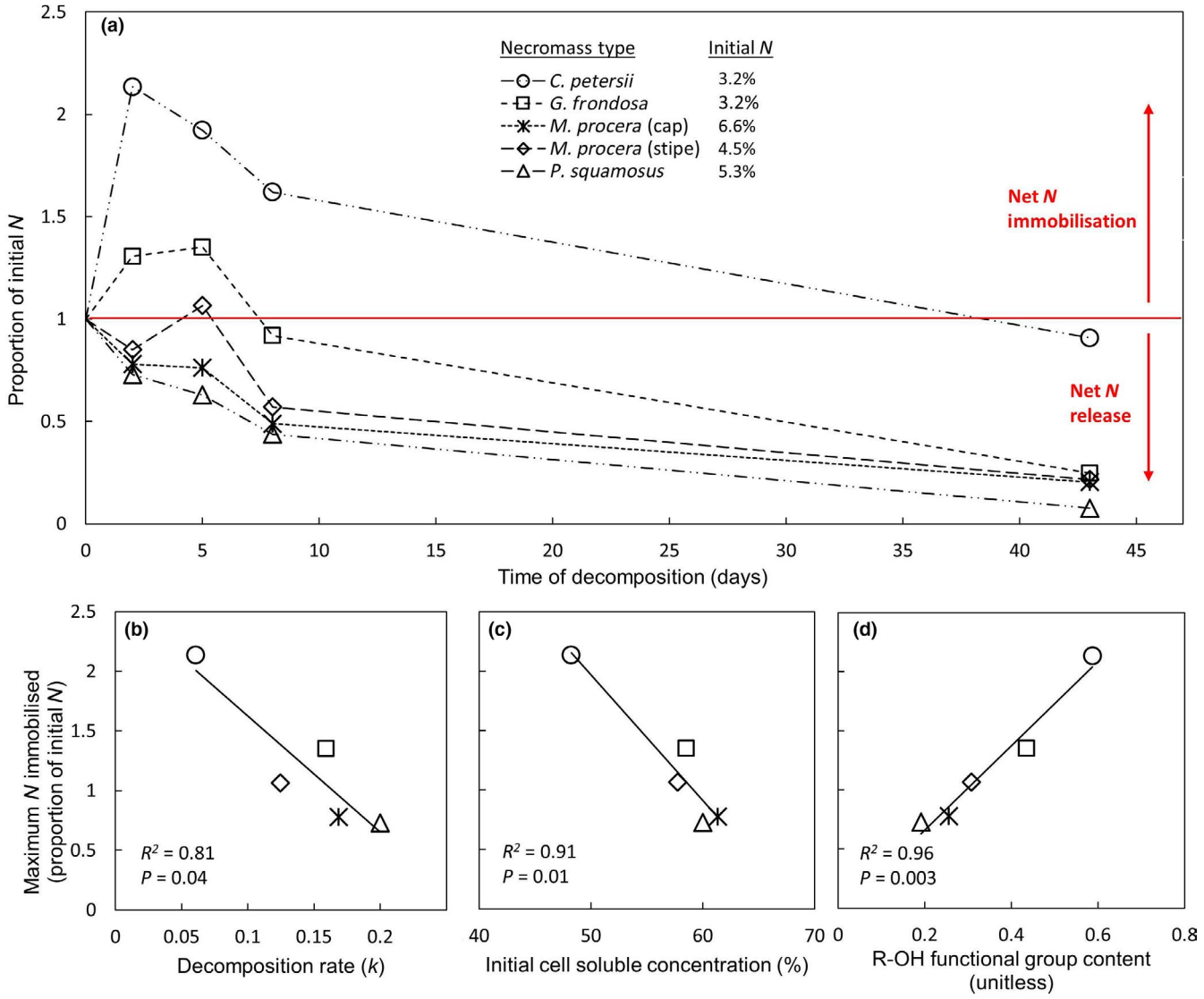

FIGURE 3 (a) Patterns of N release from decomposing fungal necromass over a 43-day period, calculated for five substrates as the proportion of the initial N pool. (b) The maximum proportion of N immobilised for each substrate over the course of decomposition declined as the decomposition rate *k* of the fast pool increased. (c) The maximum proportion of N immobilised was lower in substrates with high initial cell soluble contents. (d) Normalised R-OH bond contents (reflecting cell wall polysaccharides) estimated using peak intensity at 1,160 cm^{-1} on FTIR spectrum linearly predicted the maximum proportion of initial substrate N immobilised

altering the carbon use efficiency of the microbial communities that feed upon it (Cotrufo et al., 2013). Regardless of the mechanism, it is worth noting that the higher proportion of fast decomposing mass in fungal necromass relative to plant litter suggests that these substrates may play a disproportionate role in building stable soil C.

The role of the slow necromass pool in SOM accumulation is less clear, as its residence time has not been well quantified. Fernandez et al. (2019) found that the recalcitrant pool remained largely unchanged in litterbags for at least 2 years in a peat bog, with only negligible effects of temperature under oxic conditions. Since the litterbags in that study (53 μm mesh, placed 5 cm into *Sphagnum* spp.) prevented direct interactions with soil minerals, this pool persisted as particulate organic matter. While recent research has focused on the role of mineral associated organic matter in SOM accumulation (Lavallee et al., 2019), fungal byproducts physically stabilised as particulate matter can constitute a large proportion of SOM (Frey et al., 1999; Six et al., 2006). Melanin may be especially important to this pool, as fungal-derived melanin is prevalent in soils across systems (Van Der Wal et al., 2009), correlates with soil C stocks (Siletti et al., 2017), and has the potential to accumulate rapidly (Kallenbach et al., 2016). Because melanin is unhydrolysable even by strong acids (Bull, 1970), it is worth noting that fungal melanin is likely included in estimates of pyrogenic or 'slow-moving' soil C pools determined via acid hydrolysis (Paul et al., 2006).

4.4 | Study limitations and future directions

This study advances understanding of fungal necromass decay as it relates to substrate chemistry, but many limitations exist due to it being conducted under laboratory conditions. The soils used in our

microcosms contained an intact community of soil saprotrophs, but not active mycorrhizal fungi, which influence decomposition in the field (Frey, 2019). It is also possible that inoculating with *M. elongata* biased our results towards the enzymatic capabilities of this fungi. However, *M. elongata* is an early coloniser of necromass and is quickly outcompeted (Beidler et al., 2020; Fernandez & Kennedy, 2018), and prior work suggests it can decompose both chitin (De Boer et al., 1999) and β-glucans (Li et al., 2018), the major polysaccharides present in fungal cell walls. Finally, our results reflect decomposition dynamics from a single soil type. Biotic and abiotic differences across systems will likely to affect fungal necromass decomposition as they do plant tissues (Prescott, 2010; Veen et al., 2015). Currently, the only cross-system study of necromass decomposition found relatively small effects of edaphic factors and plant communities on the rate of fungal necromass decay, concluding that substrate chemistry was the largest driver (Beidler et al., 2020). Future field studies across a wide range of soil conditions are needed to confirm this pattern.

5 | CONCLUSIONS

Here we demonstrate strong generality of the asymptotic decomposition model for describing mass loss in fungal necromass, which occurs in two stages driven by distinctly different chemical fractions of the substrate. The fast pool constitutes the majority of fungal dry mass, and decomposes exponentially at a rate that is positively related to the mass of cell soluble contents and negatively to the mass of cell wall constituents. The size of the cell wall fraction (relative to cell soluble components) determines the rate of N release during the early stages of decomposition, and whether the necromass acts as a net source or a net sink of N during this time. The residence time of the slow decomposing fungal necromass pool remains unknown, but is composed of melanins and other aromatic, acid-unhydrolysable compounds. Beyond empirically fitting the data, the asymptotic model of decomposition implicitly acknowledges the variation in biochemistry across this diverse kingdom, allowing for better characterisation of the effects of fungal traits (e.g. melanisation, cell wall structure) on rates of soil C and N cycling.

ACKNOWLEDGEMENTS

We thank two anonymous reviewers for their excellent feedback on an earlier version of this manuscript. Hannah Vanderscheuren and Hanan Farah provided additional assistance in the laboratory. This work was funded in part by NSF DEB-1754679 to P. Kennedy, a Carleton College Externship to A. Conley and a Minnesota Mycological Society graduate research grant to C. See. The paper was written in part during C. See's residency at the Sitka Center for Arts and Ecology. This research is part of the Cedar Creek LTER Program, funded by NSF DEB-1234162 and DEB-1831944.

AUTHORS' CONTRIBUTIONS

C.R.S. and A.M.C. conceived the study and designed the methodology; A.M.C., C.R.S., K.A.H. and L.C.D. collected the data; C.R.S. and A.M.C. analysed the data; C.R.S. led the writing of the manuscript with contribution from all authors.

DATA AVAILABILITY STATEMENT

Data collected from this study are available via the Environmental Data Initiative. https://doi.org/10.6073/pasta/7173255f16bf4848fac274b50e225e2e.

ORCID

Craig R. See https://orcid.org/0000-0003-4154-8307
Chris W. Fernandez https://orcid.org/0000-0002-6310-6027
Anna M. Conley https://orcid.org/0000-0003-1759-1970
Lang C. DeLancey https://orcid.org/0000-0001-5605-5834
Katherine A. Heckman https://orcid.org/0000-0003-2265-4542
Peter G. Kennedy https://orcid.org/0000-0003-2615-3892
Sarah E. Hobbie https://orcid.org/0000-0001-5159-031X

REFERENCES

Beidler, K. V., Phillips, R. P., Andrews, E., Maillard, F., Mushinski, R. M., & Kennedy, P. G. (2020). Substrate quality drives fungal necromass decay and decomposer community structure under contrasting vegetation types. *Journal of Ecology*, *108*(5), 1845–1859. https://doi.org/10.1111/1365-2745.13385

Berg, B. (2000). Litter decomposition and organic matter turnover in northern forest soils. *Forest Ecology and Management*, *133*(1–2), 13–22. https://doi.org/10.1016/S0378-1127(99)00294-7

Boberg, J. B., Finlay, R. D., Stenlid, J., Ekblad, A., & Lindahl, B. D. (2014). Nitrogen and carbon reallocation in fungal mycelia during decomposition of boreal forest litter. *PLoS ONE*, *9*(3), e92897. https://doi.org/10.1371/journal.pone.0092897

Bowman, S. M., & Free, S. J. (2006). The structure and synthesis of the fungal cell wall. *BioEssays*, *28*, 799–808. https://doi.org/10.1002/bies.20441

Brabcová, V., Nováková, M., Davidová, A., & Baldrian, P. (2016). Dead fungal mycelium in forest soil represents a decomposition hotspot and a habitat for a specific microbial community. *New Phytologist*, *210*(4), 1369–1381. https://doi.org/10.1111/nph.13849

Bull, A. T. (1970). Chemical composition of wild-type and mutant *Aspergillus nidulans* cell walls. The nature of polysaccharide and melanin constituents. *Journal of General Microbiology*, *63*(1), 75–94. https://doi.org/10.1099/00221287-63-1-75

Butler, M. J., & Day, A. W. (1998). Fungal melanins: A review. *Canadian Journal of Microbiology*, *44*(12), 1115–1136. https://doi.org/10.1139/w98-119

Chen, J., Seven, J., Zilla, T., Dippold, M. A., Blagodatskaya, E., & Kuzyakov, Y. (2019). Microbial C:N:P stoichiometry and turnover depend on nutrients availability in soil: A ^{14}C, ^{15}N and ^{33}P triple labelling study. *Soil Biology and Biochemistry*, *131*, 206–216. https://doi.org/10.1016/j.soilbio.2019.01.017

Clemmensen, K. E., Finlay, R. D., Dahlberg, A., Stenlid, J., Wardle, D. A., & Lindahl, B. D. (2015). Carbon sequestration is related to mycorrhizal fungal community shifts during long-term succession in boreal forests. *New Phytologist*, *205*(4), 1525–1536. https://doi.org/10.1111/nph.13208

Cotrufo, M. F., Wallenstein, M. D., Boot, C. M., Denef, K., & Paul, E. (2013). The Microbial Efficiency-Matrix Stabilization (MEMS) framework integrates plant litter decomposition with soil organic matter stabilization: Do labile plant inputs form stable soil organic matter? *Global Change Biology*, *19*(4), 988–995. https://doi.org/10.1111/gcb.12113

De Boer, W., Gerards, S., Gunnewiek, P. K., & Modderman, R. (1999). Response of the chitinolytic microbial community to chitin amendments

of dune soils. *Biology and Fertility of Soils*, *29*(2), 170–177. https://doi.org/10.1007/s003740050541

Eisenman, H. C., & Casadevall, A. (2012). Synthesis and assembly of fungal melanin. *Applied Microbiology and Biotechnology*, *93*(3), 931–940. https://doi.org/10.1007/s00253-011-3777-2

Fernandez, C. W., Heckman, K., Kolka, R., & Kennedy, P. G. (2019). Melanin mitigates the accelerated decay of mycorrhizal necromass with peatland warming. *Ecology Letters*, *22*, 498–505. https://doi.org/10.1111/ele.13209

Fernandez, C. W., & Kennedy, P. G. (2018). Melanization of mycorrhizal fungal necromass structures microbial decomposer communities. *Journal of Ecology*, *106*(2), 468–479. https://doi.org/10.1111/1365-2745.12920

Fernandez, C. W., & Koide, R. T. (2012). The role of chitin in the decomposition of ectomycorrhizal fungal litter. *Ecology*, *93*(1), 24–28. https://doi.org/10.1890/11-1346.1

Fernandez, C. W., & Koide, R. T. (2014). Initial melanin and nitrogen concentrations control the decomposition of ectomycorrhizal fungal litter. *Soil Biology and Biochemistry*, *77*, 150–157. https://doi.org/10.1016/j.soilbio.2014.06.026

Fernandez, C. W., Langley, J. A., Chapman, S., McCormack, M. L., & Koide, R. T. (2016). The decomposition of ectomycorrhizal fungal necromass. *Soil Biology and Biochemistry*, *93*, 38–49. https://doi.org/10.1016/j.soilbio.2015.10.017

Fernandez, C. W., McCormack, M. L., Hill, J. M., Pritchard, S. G., & Koide, R. T. (2013). On the persistence of *Cenococcum geophilum* ectomycorrhizas and its implications for forest carbon and nutrient cycles. *Soil Biology and Biochemistry*, *65*, 141–143. https://doi.org/10.1016/j.soilbio.2013.05.022

Frey, S. D. (2019). Mycorrhizal fungi as mediators of soil organic matter dynamics. *Annual Review of Ecology, Evolution, and Systematics*, *50*, 237–259. https://doi.org/10.1146/annurev-ecolsys-110617-062331

Frey, S. D., Elliott, E. T., & Paustian, K. (1999). Bacterial and fungal abundance and biomass in conventional and no-tillage agroecosystems along two climatic gradients. *Soil Biology and Biochemistry*, *31*(4), 573–585. https://doi.org/10.1016/S0038-0717(98)00161-8

Fuss, C. B., Lovett, G. M., Goodale, C. L., Ollinger, S. V., Lang, A. K., & Ouimette, A. P. (2019). Retention of nitrate-N in mineral soil organic matter in different forest age classes. *Ecosystems*, *22*(6), 1280–1294. https://doi.org/10.1007/s10021-018-0328-z

Grigal, D. F., Finney, H. R., Wroblewski, D. V., & Gross, E. V. (1974). *Soils of the Cedar Creek Natural History Area*. Agricultural Experiment Station, University of Minnesota.

Hobbie, E. A., Sánchez, F. S., & Rygiewicz, P. T. (2012). Controls of isotopic patterns in saprotrophic and ectomycorrhizal fungi. *Soil Biology and Biochemistry*, *48*, 60–68. https://doi.org/10.1016/j.soilbio.2012.01.014

Hobbie, S. E., Oleksyn, J., Eissenstat, D. M., & Reich, P. B. (2010). Fine root decomposition rates do not mirror those of leaf litter among temperate tree species. *Oecologia*, *162*(2), 505–513. https://doi.org/10.1007/s00442-009-1479-6

Howard, P. J. A., & Howard, D. M. (1974). Microbial decomposition of tree and shrub leaf litter. 1. Weight loss and chemical composition of decomposing litter. *Oikos*, *25*(3), 341. https://doi.org/10.2307/3543954

Hribljan, J. A., Kane, E. S., & Chimner, R. A. (2017). Implications of altered hydrology for substrate quality and trace gas production in a poor fen peatland. *Soil Science Society of America Journal*, *81*(3), 633–646. https://doi.org/10.2136/sssaj2016.10.0322

Jang, M.-K., Kong, B.-G., Jeong, Y.-I., Lee, C. H., & Nah, J.-W. (2004). Physicochemical characterization of α-chitin, β-chitin, and γ-chitin separated from natural resources. *Journal of Polymer Science Part A: Polymer Chemistry*, *42*(14), 3423–3432. https://doi.org/10.1002/pola.20176

Kallenbach, C. M., Frey, S. D., & Grandy A. S. (2016). Direct evidence for microbial-derived soil organic matter formation and its ecophysiological controls. *Nature Communications*, *7*(1). https://doi.org/10.1038/ncomms13630

Koide, R. T., & Malcolm, G. M. (2009). N concentration controls decomposition rates of different strains of ectomycorrhizal fungi. *Fungal Ecology*, *2*(4), 197–202. https://doi.org/10.1016/j.funeco.2009.06.001

Lavallee, J. M., Soong, J. L., & Cotrufo M. F. (2020). Conceptualizing soil organic matter into particulate and mineral-associated forms to address global change in the 21st century. *Global Change Biology*, *26*(1), 261–273. https://doi.org/10.1111/gcb.14859

Lenaers, M., Reyns, W., Czech, J., Carleer, R., Basak, I., Deferme, W., Krupinska, P., Yildiz, T., Saro, S., Remans, T., Vangronsveld, J., De Laender, F., & Rineau, F. (2018). Links between heathland fungal biomass mineralization, melanization, and hydrophobicity. *Microbial Ecology*, *76*(3), 762–770. https://doi.org/10.1007/s00248-018-1167-3

Li, F., Chen, L., Redmile-Gordon, M., Zhang, J., Zhang, C., Ning, Q., & Li, W. (2018). *Mortierella elongata*'s roles in organic agriculture and crop growth promotion in a mineral soil. *Land Degradation & Development*, *29*(6), 1642–1651. https://doi.org/10.1002/ldr.2965

Liang, C., Amelung, W., Lehmann, J., & Kästner, M. (2019). Quantitative assessment of microbial necromass contribution to soil organic matter. *Global Change Biology*, *25*(11), 3578–3590. https://doi.org/10.1111/gcb.14781

López-Mondéjar, R., Brabcová, V., Štursová, M., Davidová, A., Jansa, J., Cajthaml, T., & Baldrian, P. (2018). Decomposer food web in a deciduous forest shows high share of generalist microorganisms and importance of microbial biomass recycling. *ISME Journal*, *12*(7), 1768–1778. https://doi.org/10.1038/s41396-018-0084-2

Lousier, J. D., & Parkinson, D. (1976). Litter decomposition in a cool temperate deciduous forest. *Canadian Journal of Botany*, *54*(5–6), 419–436. https://doi.org/10.1139/b76-041

Lovett, G. M., Goodale, C. L., Ollinger, S. V., Fuss, C. B., Ouimette, A. P., & Likens, G. E. (2018). Nutrient retention during ecosystem succession: A revised conceptual model. *Frontiers in Ecology and the Environment*, *16*(9), 532–538. https://doi.org/10.1002/fee.1949

Ludwig, M., Achtenhagen, J., Miltner, A., Eckhardt, K. U., Leinweber, P., Emmerling, C., & Thiele-Bruhn, S. (2015). Microbial contribution to SOM quantity and quality in density fractions of temperate arable soils. *Soil Biology and Biochemistry*, *81*, 311–322. https://doi.org/10.1016/j.soilbio.2014.12.002

Maillard, F., Schilling, J., Andrews, E., Schreiner, K. M., & Kennedy, P. (2020). Functional convergence in the decomposition of fungal necromass in soil and wood. *FEMS Microbiology Ecology*, *96*(2), 1–13. https://doi.org/10.1093/femsec/fiz209

Margenot, A. J., Calderón, F. J., Bowles, T. M., Parikh, S. J., & Jackson, L. E. (2015). Soil organic matter functional group composition in relation to organic carbon, nitrogen, and phosphorus fractions in organically managed tomato fields. *Soil Science Society of America Journal*, *79*(3), 772–782. https://doi.org/10.2136/sssaj2015.02.0070

Miltner, A., Bombach, P., Schmidt-Brücken, B., & Kästner, M. (2012). SOM genesis: Microbial biomass as a significant source. *Biogeochemistry*, *111*(1–3), 41–55. https://doi.org/10.1007/s10533-011-9658-z

Nosanchuk, J. D., Stark, R. E., & Casadevall, A. (2015). Fungal melanin: What do we know about structure? *Frontiers in Microbiology*, *6*, 01463. https://doi.org/10.3389/fmicb.2015.01463

Olson, J. S. (1963). Energy storage and the balance of producers and decomposers in ecological systems. *Ecology*, *44*(2), 322–331. https://doi.org/10.2307/1932179

Parton, W., Silver, W. L., Burke, I. C., Grassens, L., Harmon, M. E., Currie, W. S., King, J. Y., Adair, E. C., Brandt, L. A., Hart, S. C., & Fasth, B. (2007). Global-scale similarities in nitrogen release patterns during long-term decomposition. *Science*, *315*, 361–364. https://doi.org/10.1126/science.1134853

Paul, E. A., Morris, S. J., Conant, R. T., & Plante, A. F. (2006). Does the acid hydrolysis-incubation method measure meaningful soil organic

carbon pools? *Soil Science Society of America Journal*, *70*(3), 1023–1035. https://doi.org/10.2136/sssaj2005.0103

Prescott, C. E. (2010). Litter decomposition: What controls it and how can we alter it to sequester more carbon in forest soils? *Biogeochemistry*, *101*, 133–149. https://doi.org/10.1007/s10533-010-9439-0

Ryan, M. E., Schreiner, K. M., Swenson, J. T., Gagne, J., & Kennedy, P. G. (2020). Rapid changes in the chemical composition of degrading ectomycorrhizal fungal necromass. *Fungal Ecology*, *45*, 100922. https://doi.org/10.1016/j.funeco.2020.100922

Schweigert, M., Herrmann, S., Miltner, A., Fester, T., & Kästner, M. (2015). Fate of ectomycorrhizal fungal biomass in a soil bioreactor system and its contribution to soil organic matter formation. *Soil Biology and Biochemistry*, *88*, 120–127. https://doi.org/10.1016/j.soilbio.2015.05.012

Scott, A. C., Pinter N., Collinson, Margaret E., Hardiman, M., Anderson, R. S., Brain, A. P. R., Smith, S. Y., Marone, F., & Stampanoni M. (2010). Fungus, not comet or catastrophe, accounts for carbonaceous spherules in the Younger Dryas "impact layer". *Geophysical Research Letters*, *37*(14). https://doi.org/10.1029/2010gl043345

Shao, P., Liang, C., Lynch, L., Xie, H., & Bao, X. (2019). Reforestation accelerates soil organic carbon accumulation: Evidence from microbial biomarkers. *Soil Biology and Biochemistry*, *131*, 182–190. https://doi.org/10.1016/j.soilbio.2019.01.012

Siletti, C. E., Zeiner, C. A., & Bhatnagar, J. M. (2017). Soil Biology & Biochemistry Distributions of fungal melanin across species and soils. *Soil Biology and Biochemistry*, *113*, 285–293. https://doi.org/10.1016/j.soilbio.2017.05.030

Simpson, A. J., Simpson, M. J., Smith, E., & Kelleher, B. P. (2007). Microbially derived inputs to soil organic matter: Are current estimates too low? *Environmental Science and Technology*, *41*(23), 8070–8076. https://doi.org/10.1021/es071217x

Sinsabaugh, R. L., Carreiro, M. M., & Repert, D. A. (2002). Allocation of extracellular enzymatic activity in relation to litter composition, N deposition, and mass loss. *Biogeochemistry*, *60*, 1–24. https://doi.org/10.2307/1469657

Six, J., Frey, S. D., Thiet, R. K., & Batten, K. M. (2006). Bacterial and fungal contributions to carbon sequestration in agroecosystems. *Soil Science Society of America Journal*, *70*(2), 555–569. https://doi.org/10.2136/sssaj2004.0347

Sulman, B. N., Brzostek, E. R., Medici, C., Shevliakova, E., Menge, D. N. L., & Phillips, R. P. (2017). Feedbacks between plant N demand and rhizosphere priming depend on type of mycorrhizal association. *Ecology Letters*, *20*(8), 1043–1053. https://doi.org/10.1111/ele.12802

Sulman, B. N., Phillips, R. P., Oishi, A. C., Shevliakova, E., & Pacala, S. W. (2014). Microbe-driven turnover offsets mineral-mediated storage of soil carbon under elevated CO_2. *Nature Climate Change*, *4*(12), 1099–1102. https://doi.org/10.1038/nclimate2436

Van Der Wal, A., Bloem, J., Mulder, C., & De Boer, W. D. (2009). Soil Biology & Biochemistry Relative abundance and activity of melanized hyphae in different soil ecosystems. *Soil Biology and Biochemistry*, *41*(2), 417–419. https://doi.org/10.1016/j.soilbio.2008.10.031

Veen, G. F. C., Freschet, G. T., Ordonez, A., & Wardle, D. A. (2015). Litter quality and environmental controls of home-field advantage effects on litter decomposition. *Oikos*, *124*(2), 187–195. https://doi.org/10.1111/oik.01374

Wieder, R. K., & Lang, G. E. (1982). A critique of the analytical methods used in examining decomposition data obtained from litter bags. *Ecology*, *63*(6), 1636–1642. https://doi.org/10.2307/1940104

Wieder, W. R., Allison, S. D., Davidson, E. A., Georgiou, K., Hararuk, O., He, Y., Hopkins, F., Luo, Y., Smith, M. J., Sulman, B., Todd-Brown, K., Wang, Y.-P., Xia, J., & Xu, X. (2015). Explicitly representing soil microbial processes in Earth system models. *Global Biogeochemical Cycles*, *29*(10), 1782–1800. https://doi.org/10.1002/2015GB005188

Wieder, W. R., Cleveland, C. C., Townsend, A. R., Wieder, W. R., Cleveland, C. C., & Townsend, A. R. (2009). Controls over leaf litter decomposition in wet tropical forests. *Ecology*, *90*(12), 3333–3341. https://doi.org/10.1890/08-2294.1

SUPPORTING INFORMATION

Additional supporting information may be found online in the Supporting Information section.

How to cite this article: See CR, Fernandez CW, Conley AM, et al. Distinct carbon fractions drive a generalisable two-pool model of fungal necromass decomposition. *Funct Ecol*. 2021;35:796–806. https://doi.org/10.1111/1365-2435.13728